Development of a middle-range six-degrees-of-freedom system

W Jywe[1]*, Y-R Jeng[2], C-H Liu[3], Y-F Teng[2], C-H Wu[4], T-H Hsieh[5], and **L-L Duan[1]**
[1]Department of Automation Engineering, National Formosa University, Huwei, Taiwan, Republic of China
[2]Department of Mechanical Engineering, National Chung Cheng University, Chia-Yi, Taiwan, Republic of China
[3]Institute of Electro-Optical and Materials Science, National Formosa University, Huwei, Taiwan, Republic of China
[4]Department of Mechanical Engineering, National Cheng Kung University, Tainan, Taiwan, Republic of China
[5]Institute of Mechanical and Electro-Mechanical Engineering, National Formosa University, Huwei, Taiwan, Republic of China

The manuscript was received on 29 November 2008 and was accepted after revision for publication on 7 September 2010.

DOI: 10.1243/09544054JEM1436

Abstract: This paper describes the successful development of a middle-range six-degrees-of-freedom stage, using the features of a flexible structure. The system includes two parts: a middle-range positioning *X*–*Y* stage and a four-degrees-of-freedom stage. The flexible structure of the four-degrees-of-freedom stage is built from two kinds of flexible bodies: circular hinges and a new two-degrees-of-freedom flexible body. The four-degrees-of-freedom stage was designed to compensate movement errors including linear displacement, pitch, and roll errors. The linear displacement reaches 20 mm along the *X*-axis, 20 mm along the *Y*-axis, and 5 μm along the *Z*-axis. The rotation angle around the *X*-axis (θ_x), *Y*-axis (θ_y), and *Z*-axis (θ_z) were all 10 arcsec. A novel six-degrees-of-freedom measuring system was also designed. Precision feedback control is demonstrated in a series of experiments performed using the proposed measurement system.

Keywords: stack-type stage, flexure hinge, nanometre stage, piezoelectric, positioning control

1 INTRODUCTION

The development of precision machines is important to the study of nanometre-scale manufacturing and research. Ultra-precision stage positioning and nano-measurement technology are two key points in the domain of nanotechnology. For an ultra-precision positioning stage to achieve nanometre accuracy, piezoelectric actuators are commonly used because they have nanometre resolution. In 1987, Matey *et al.* [**1**] developed an *X*–*Y*–*Z* scanning stage for a mechanically scanned microscope. The stage was constructed of 'double-S' mode piezoelectric bimorphs. The prototype unit had a deflection sensitivity of 0.3 μm/V and travelled a distance of ±60 μm. Heil *et al.* [**2**] designed a three-dimensional cryogenic micropositioner which was based on a parallelogram structure that was constructed from leaf springs and wires. The actuation was achieved by the elastic deformation of the parallelogram using screws. The precision and reproducibility of positioning were in the micrometre range. Chang and Du [**3**] designed and built a micropositioning stage with longer travel distances. The stage consisted of a piezoelectric driving element, flexure-pivoted multiple Scott–Russell linkages, and a parallel guiding spring. The experiment showed that the stage was a vacuum-compatible device and had a travel distance of greater than 100 μm, with a resolution of 0.04 μm, and an angular deviation of less than 31.1 μrad. Chang *et al.* [**4**–**5**] designed a novel three-degrees-of-freedom micropositioner using a monolithic flexural mechanism with built-in multilayer piezoelectric actuators and sensors to achieve the translations in the *X*- and *Y*-axis directions and rotation in the θ_z -axis direction. Jywe *et al.* [**6**, **7**] used the features of a flexible structure to develop a stack-type

**Corresponding author: Department of Automation Engineering, National Formosa University, 64 Wenhua Road, Huwei, Huwei 632, Taiwan, Republic of China.*
email: jywe@sunws.nfu.edu.tw

nanometre positioning stage with five-degrees-of-freedom for a heavy loading which allowed the increase or decrease of axis action movement in accordance with various needs. The development of a long-range ultra-precision positioning stage has become an important target in the field of nanometre science and technology. Micropositioning stages with large travel ranges have been developed [**8**–**11**]. These stages combine generally a piezoelectric driving element, flexure-pivoted multiple Scott–Russell linkages, and a parallel guiding spring. Nowadays, precision nanometre stages are used in applications such as atomic force microscopy (AFM), scanning probe microscopy (SPM), and photolithography. Holmes *et al.* [**8**] developed a magnetically suspended six-degrees-of freedom precision motion control stage. The stage utilized four levitation linear motors to suspend and serve drive the moving element throughout its $25\times25\times0.1$ mm travel range. Jäger *et al.* [**12**] developed a nano positioning and nano measuring machine that used two voice coil motors to push the stage and three piezoelectric actuators to make the stage rise or make angular motions. The travel range was $25\times25\times5$ mm and the position accuracy was ±5 nm.

The development of a flexure hinge-based middle-range six-degrees-of-freedom stage is described in this paper. In order to simplify the structure of the stage, circular hinges and a two-degrees-of-freedom flexible body act as the main structural elements of the designed stage. Thus, the designed stage can be integrated as the final stage into a two-stage long-range ultra-positioning stage. A measuring system with multiple capacitance sensors for simultaneously measuring the multi-degrees-of-freedom motion errors is designed and integrated into the stage. Thus, precision positioning feedback can be obtained from the capacitance sensors.

2 THE STRUCTURE OF THE MIDDLE-RANGE SIX-DEGREES-OF-FREEDOM SYSTEM

This middle-range six-degrees-of-freedom system consists of two parts: a middle-range positioning *X*–*Y* stage and a four degrees-of-freedom stage. The structure of the middle-range six-degrees-of-freedom stage is shown in Fig. 1.

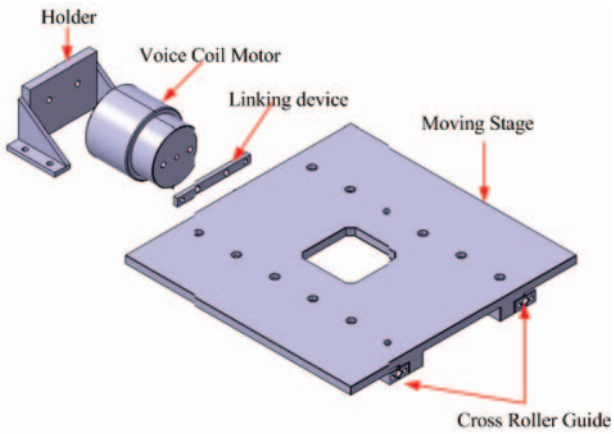

Fig. 2 The assembly process of the moving stage

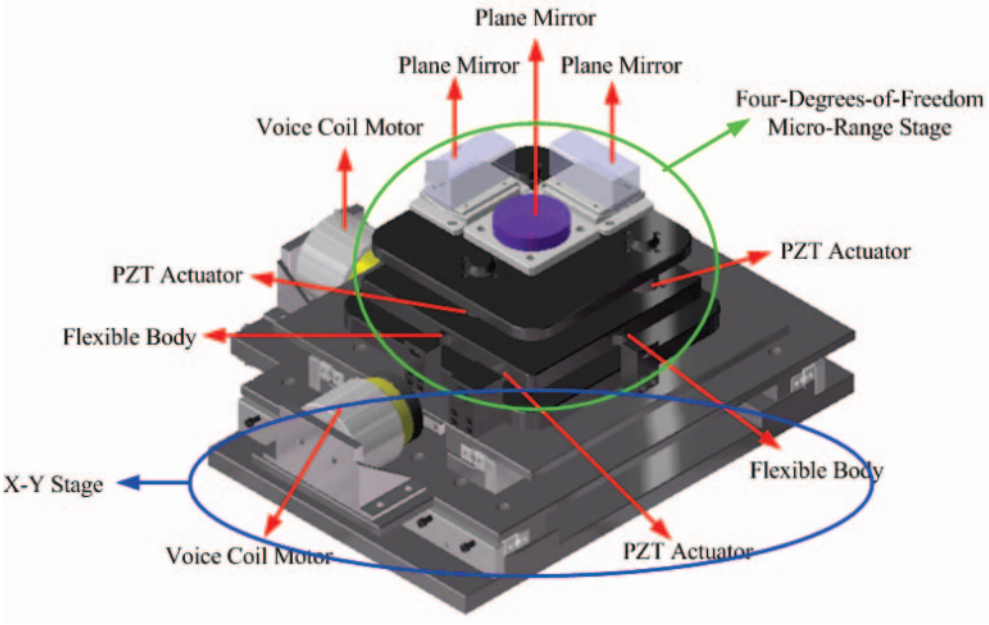

Fig. 1 The structure of the middle-range six-degrees-of-freedom system

2.1 Middle-range positioning *X–Y* stage

The middle-range positioning *X–Y* stage consists of two voice coil motors, two linear guides, a holder, a linking device, and a moving stage. The assembly process of the long-range positioning *X–Y* stage is shown in Fig. 2. The middle-range positioning *X–Y* stage is shown in Fig. 3.

2.2 The four-degrees-of-freedom stage

The four-degrees-of-freedom stage is provided with a flexible structure created by the work, use of circular hinges, and a new two-degrees-of-freedom flexible body that contains the actuator. The basic structures are shown in Fig. 4. Figure 5 shows the structure of the assembled four-degrees-of-freedom stage. The flexible structures used to create the four-degrees-of-freedom stage, were produced using by a pre-baking process. The assembled stage consists of five piezoelectric actuators, four circular hinges, three two-degrees-of-freedom flexible bodies, and a rigid base. The four-degrees-of-freedom stage allows one translational and three rotational motions that are driven by the five piezoelectric actuators – translation motion along the *Z*-axis and rotational motion about the *X*-axis (θ_x), *Y*-axis (θ_y), and *Z*-axis (θ_z).

2.3 The assembly of the middle-range six-degrees-of-freedom system

The assembly process of the middle-range six-degrees-of-freedom system, shown in Fig. 6, Fig. 7, and Fig. 8, consists of three phases. In the first part (see Fig. 6), the two-degrees-of-freedom flexible body and the piezoelectric actuator are assembled. The piezoelectric actuator is also placed into the holder and integrated with the adjustment mechanism. The adjustment mechanism supplies the preload to the piezoelectric actuators. The three-degrees-of-freedom flexible stage is created by using three two-degrees-of-freedom flexible bodies, three Lead Zirconium Titanate (PZT) actuators, holders, and adjustment mechanisms. Finally, the three-degrees-of-freedom flexible stage and rotational stage are assembled together. The rotational stage is assembled using the hinges and PZT actuators. When the two PZT actuators apply a force to the structure, the stage produces a rotational angle (θ_z). The second assembly process (see Fig. 7) concerns the creation of the *X–Y* stage from the voice coil motor and the cross roller guide. In the final assembly process (see Fig. 8), the four-degrees-of-freedom stage and the *X–Y* stage are combined to create the middle-range six-degrees-of-freedom system. Figure 9 is a photograph of the fully assembled system.

3 A SIX-DEGREES-OF-FREEDOM MEASURING SYSTEM

A six-degrees-of-freedom measuring system was designed to evaluate the performance of the

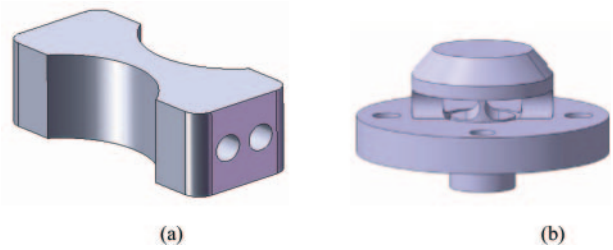

Fig. 4 The structure of the flexible bodies (a) the circular hinges, and (b) the two-degrees-of-freedom flexible body

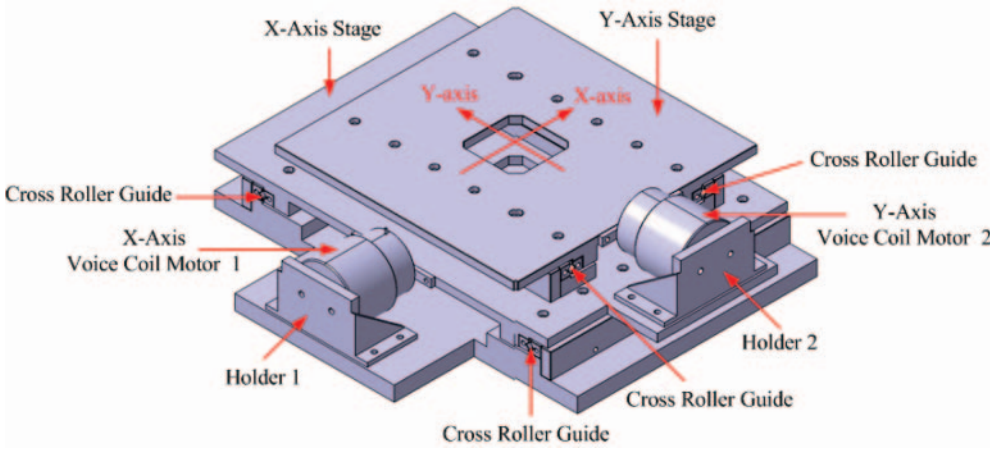

Fig. 3 The middle-range positioning *X–Y* stage

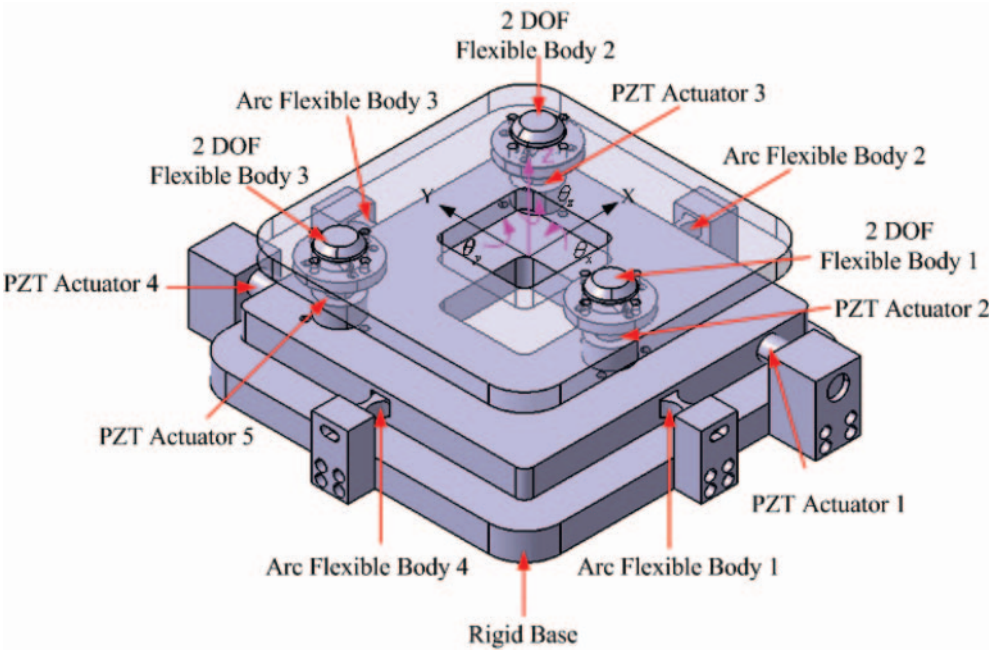

Fig. 5 The structure of the assembled four-degrees-of-freedom stage

proposed middle-range six-degrees-of-freedom system. The results obtained using this system can be used in the design of a closed-loop controller. The six-degrees-of-freedom measuring system, shown in Fig. 10, is able to measure the displacements in the *X*-axis, *Y*-axis, and *Z*-axis directions and rotational motions about the *X*-axis (θ_x), *Y*-axis (θ_y), and *Z*-axis (θ_z). In order to reduce measurement errors great care must be taken in setting up the system and in particular attention must be paid to ensure that the measuring optical axis is parallel to the moving axis. The measuring system consists of two single-beam laser interferometers (SL1 and SL2), a double-beam laser interferometer (DL1), a beam splitter (BS1), a focus lens (L1), a quadrant photo detector (QD1), and four plane mirrors (PM1, PM2, PM3, and PM4). The displacement in the *X*-axis direction can be easily measured using this system. When the stage moves, it usually produces a roll angle along the *Z*-axis direction. The rotational angle error can also be measured using the measuring system along the *X*-axis direction. The measuring principle for displacements along the *X*-axis is shown in Fig. 11. The measuring system, shown in Fig. 12, is able to measure displacements along the *Y*-axis. Displacements along the *Z*-axis can be measured using the single-beam laser interferometer (SL2). The set up for these measurements is shown in Fig. 13. The laser beam from the single-beam laser interferometer (SL2) is projected onto plane mirror PM4 and is reflected onto mirror PM3 and then onto the beam splitter (BS1) where it is divided into two parts. One beam passes through BS1 and is projected onto the receiver of the single-beam laser interferometer (SL2). The other beam is reflected by the beam splitter (BS1) and is projected onto a lens (L1) which focuses the beam onto the quadrant photo detector (QD1) to allow measurement of the pitch and the yaw errors.

4 THE CONTROL SYSTEM

The control system is shown in Fig. 14. It consists of a personal computer, a Dspace card (DS1103), an analogue amplifier (SVR 150/3), five PZT actuators (PSt150/7/20 Vs12), an elmo driver, a signal amplifier (OT301), two voice coil motors, a laser signal processor, the six-degrees-of-freedom measuring system, and the middle-range six-degrees-of-freedom stage.

A two-step control method is used in the experiments. In the first step, the motion control is at the micrometre level and in the second step it is at the nanometre level. In the first step, software is used to create the control blocks and compile the digital signal processor (DSP) card (DS1103). The DSP card then sends the control signal to the elmo driver which drives the voice coil motor that moves the *X*–*Y* stage to the correct displacement. When the *X*–*Y* stage has finished moving the DSP card sends a control signal to the amplifier (SVR 150/3), which supplies the required voltage to the piezoelectric actuators (PSt150/7/20 Vs12) of the

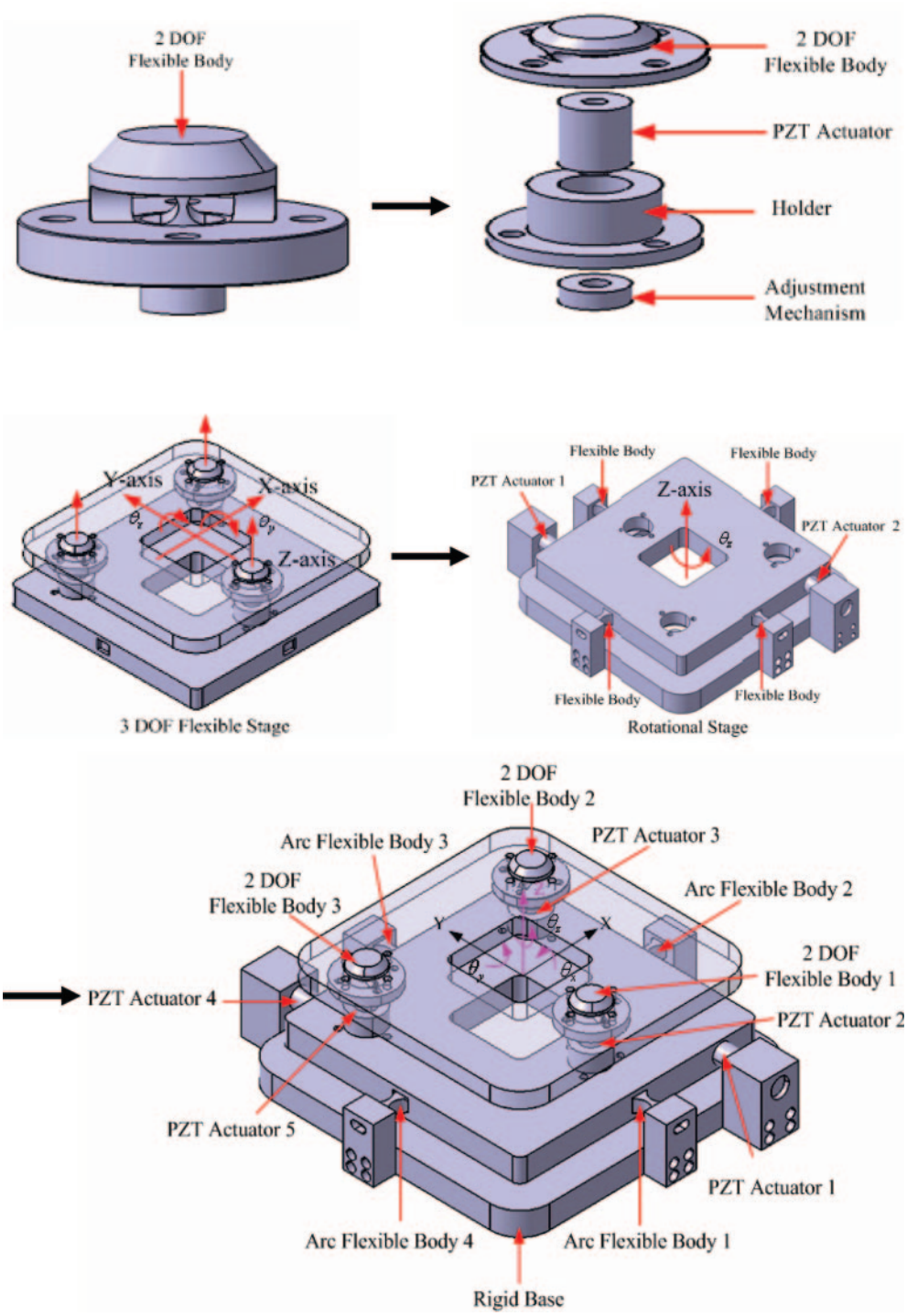

Fig. 6 The assembly process of the four-degrees-of-freedom stage

four degrees-of-freedom stage which rotates the *X*–*Y* stage. The axial displacement and the rotational angle of the middle-range six-degrees-of-freedom system created by the control actions can be measured using the six-degrees-of-freedom measuring system and this is reported in the next section.

5 THE EXPERIMENTAL PERFORMANCE OF THE MIDDLE-RANGE SIX-DEGREES-OF-FREEDOM SYSTEM

The experimental measurement system is shown in Fig. 15. It consists of two single-beam laser interferometers, one double-beam laser interferometer,

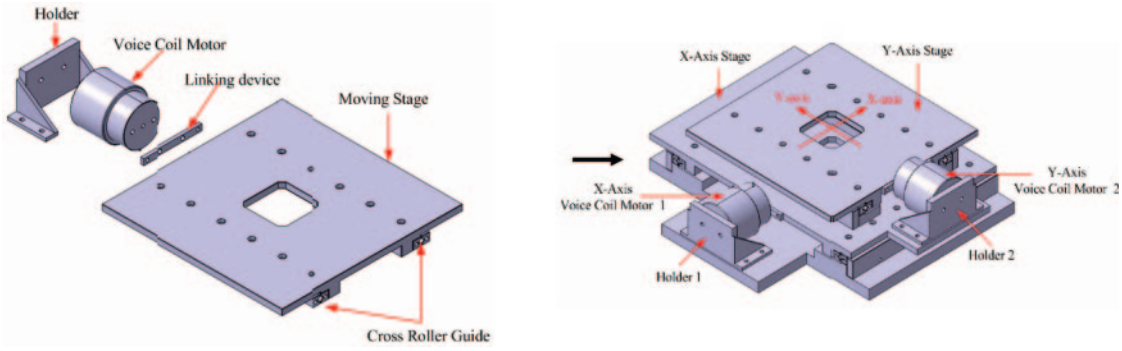

Fig. 7 The assembly process of the *X*–*Y* stage

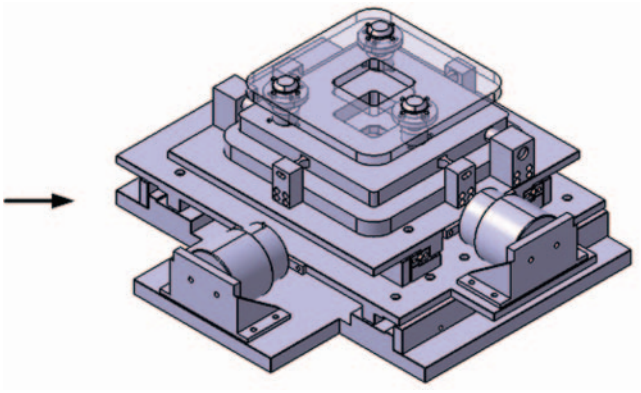

Fig. 8 The completed middle-range six-degrees-of-freedom system

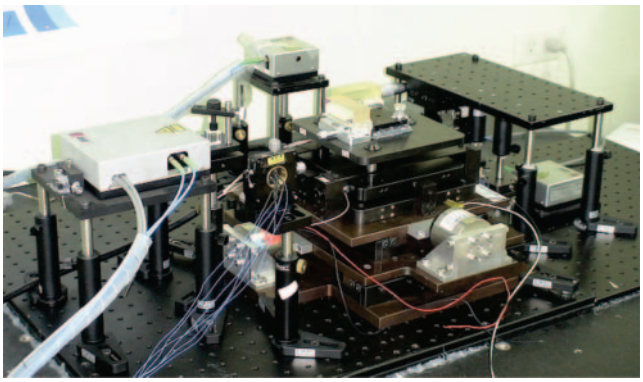

Fig. 9 Photograph of the middle-range six-degrees-of-freedom system

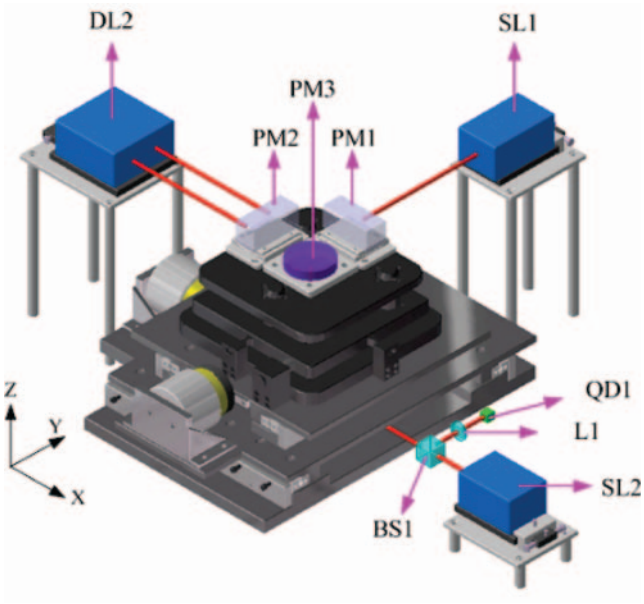

Fig. 10 The six-degrees-of-freedom measuring system

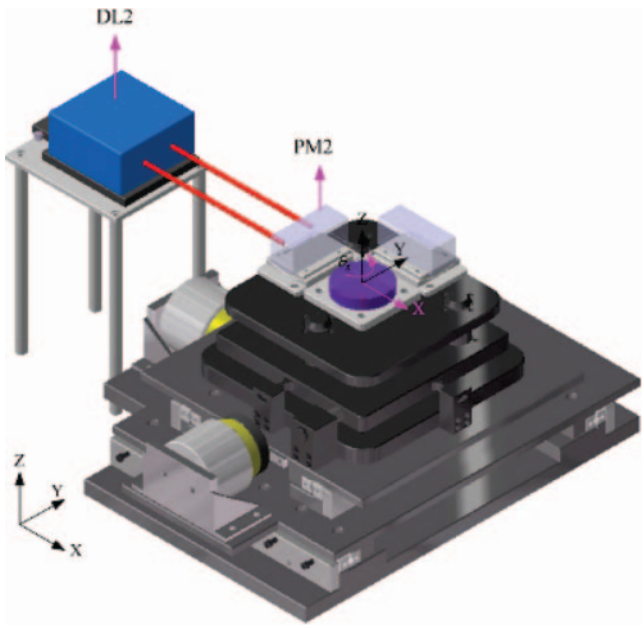

Fig. 11 The measuring principle for displacements along the *X*-axis

one beam splitter, one focus lens, one quadrant photo detector, and four plane mirrors.

Actuation of this system was done with two voice coil motors and five piezoelectric actuators. The proposed six-degrees-of-freedom measuring system was used for the position measurements. The travel range was 25 mm × 25mm × 5 μm. In the experiments, a 1 mm step signal was used to test

the performance along the *X*-axis and *Y*-axis. The experimental results are shown in Figs 16 to 19. Comparing Figs 16 and 18, it is clear that the rise time along the *X*-axis is better than that along the *Y*-axis. The performance errors of the *X*-axis and *Y*-axis are ±40 nm, ±100 nm respectively. A 500 nm step signal was used to test the performance along the *Z*-axis. The results are shown in Fig. 20 and Fig. 21. In this case the performance error is ± 5 nm. The performance for the rotational angle along the *X*-axis (θ_x), *Y*-axis (θ_y), and *Z*-axis (θ_z) was also tested. The experimental results are shown in Figs 22 to 27. The performance errors of the rotational angle along the *X*-axis (θ_x), *Y*-axis (θ_y), and *Z*-axis (θ_z) are ±0.07, ±0.08, and ±0.08 arcsec respectively.

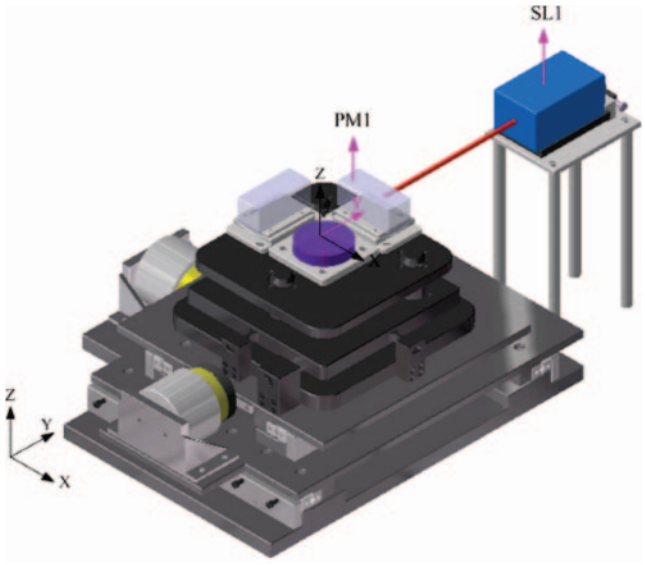

Fig. 12 The measuring principle for displacements along the *Y*-axis

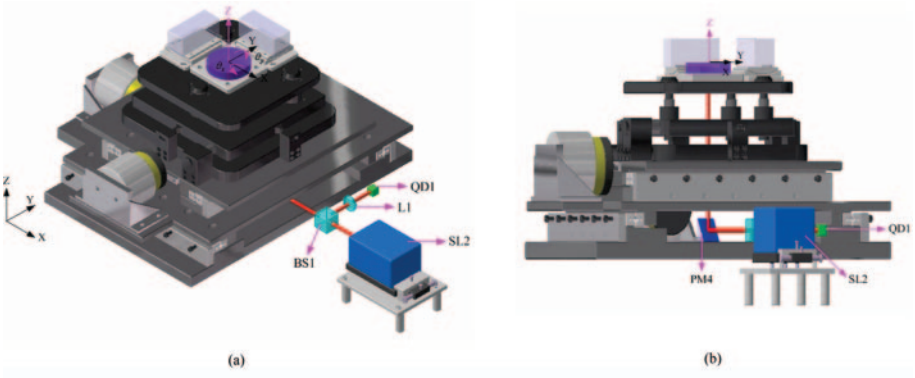

Fig. 13 The measuring principle for displacements along the *Z*-axis and the angle (a) External view (b) The internal setup

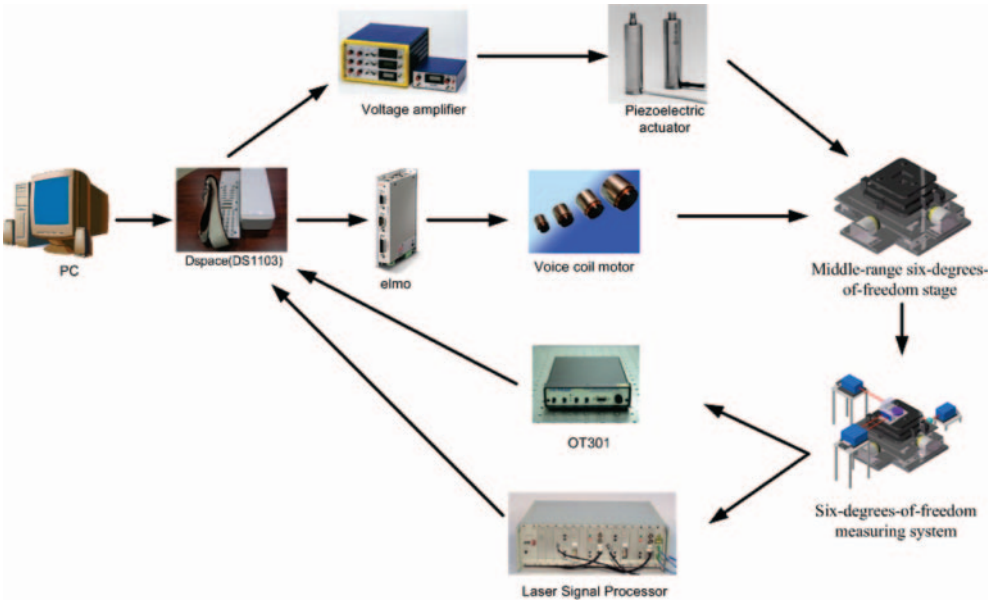

Fig. 14 Flow diagram of the control system

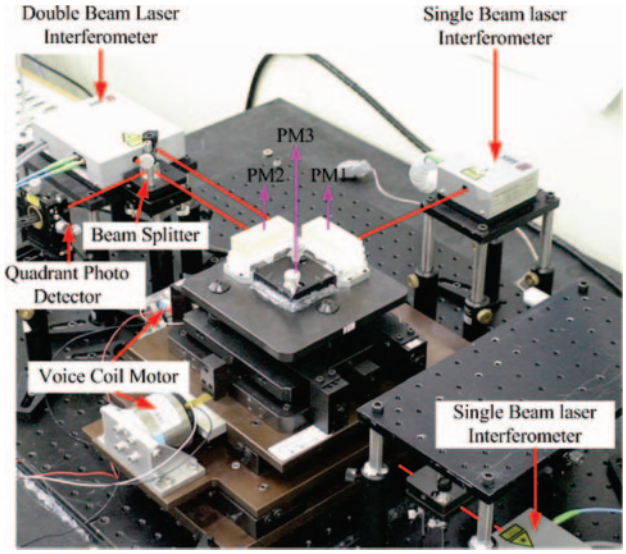

Fig. 15 The experimental measurement system

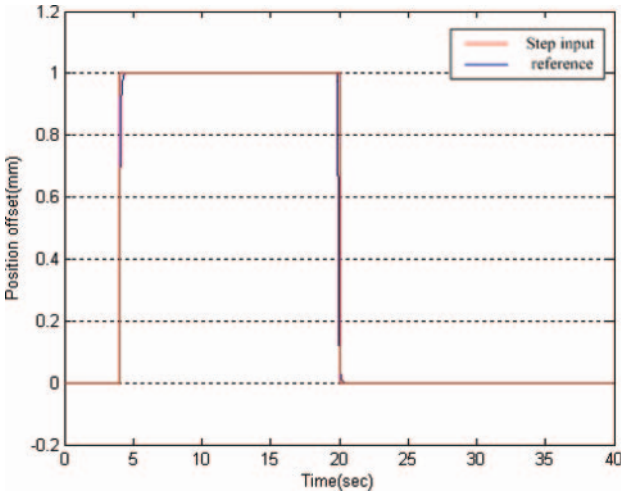

Fig. 16 The *X*-axis performance result of the step response test

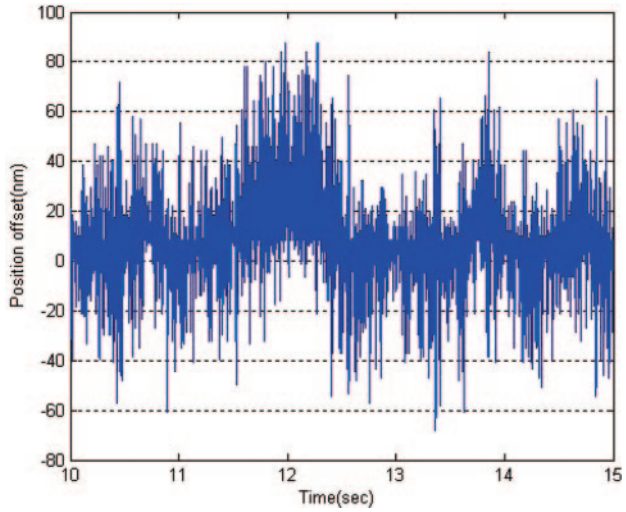

Fig. 17 The *X*-axis performance error of the step response test

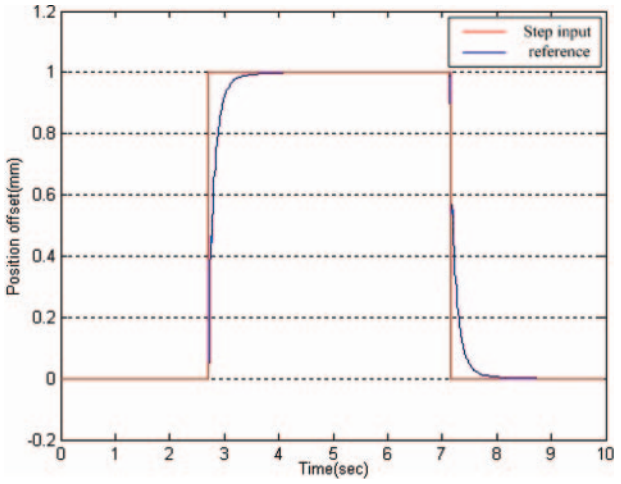

Fig. 18 The *Y*-axis performance result of the step response test

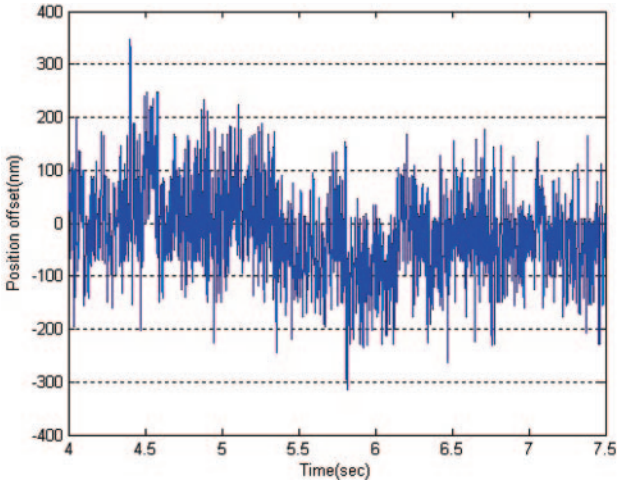

Fig. 19 The *Y*-axis performance error of the step response test

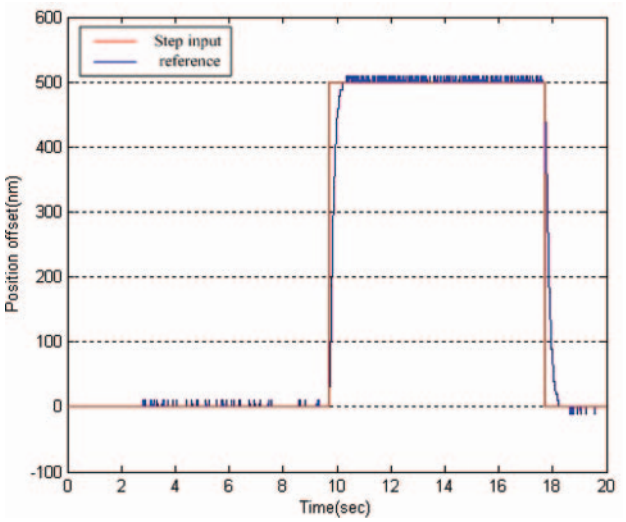

Fig. 20 The *Z*-axis performance result of the step response test

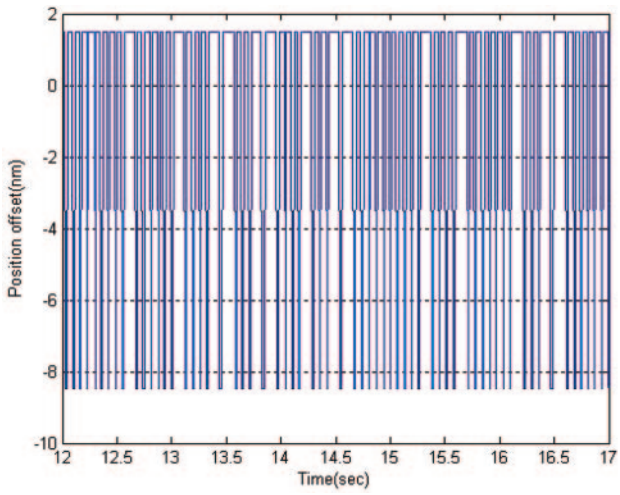

Fig. 21 The Z-axis performance error of the step response test

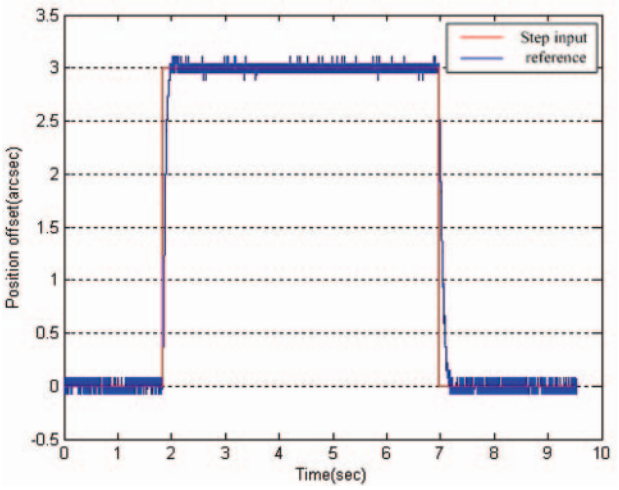

Fig. 22 The step input performance of the rotational angle θ_x

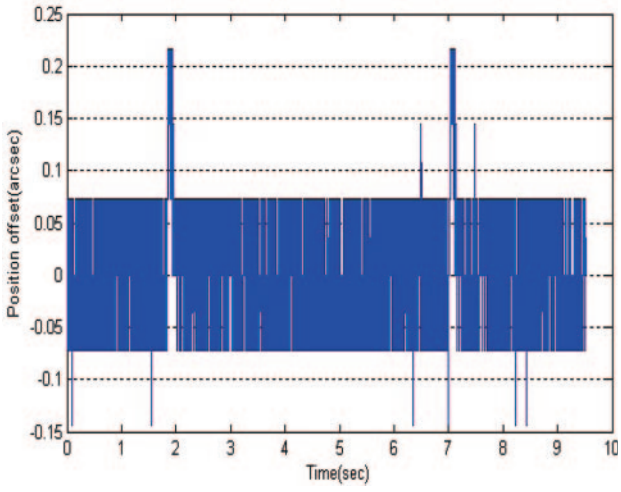

Fig. 23 The performance error of the rotational angle θ_x

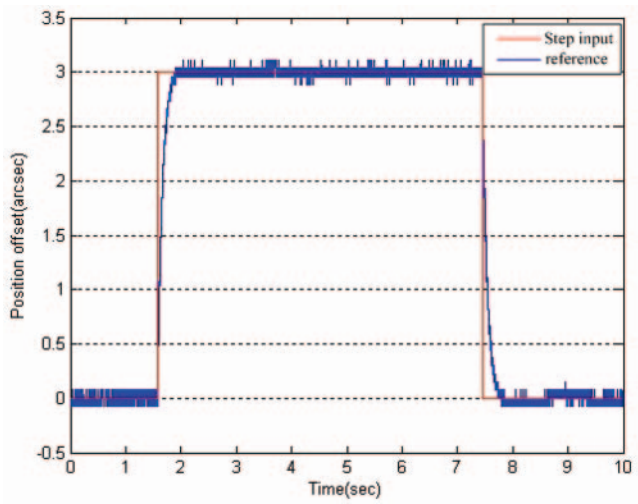

Fig. 24 The step input performance of the rotational angle θ_y

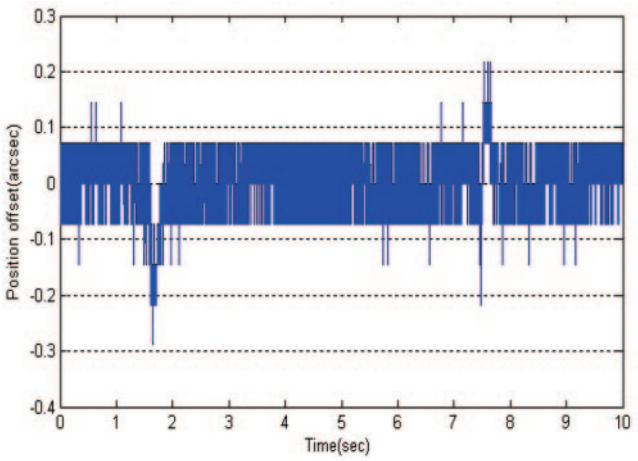

Fig. 25 The performance error of the rotational angle θ_y

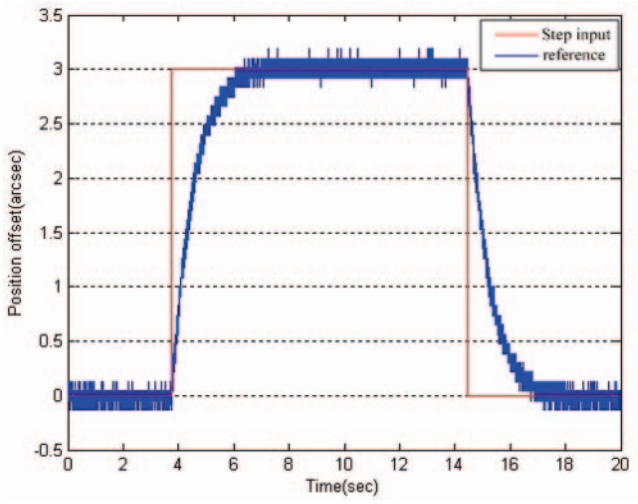

Fig. 26 The step input performance of the rotational angle θ_z

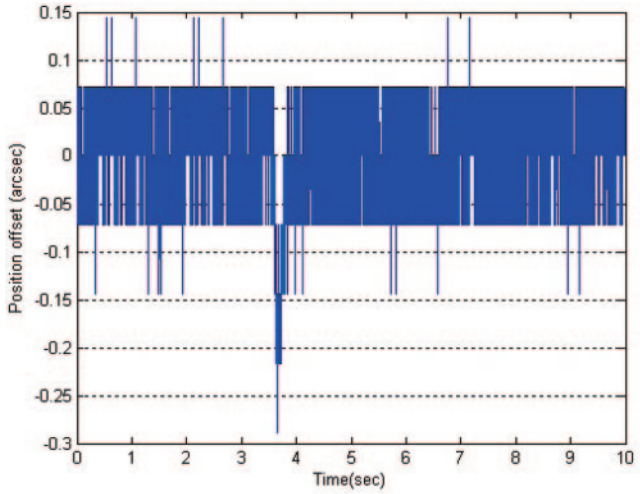

Fig. 27 The performance error of the rotational angle θ_z

6 CONCLUSION

This paper has described the successful design of a four-degrees-of-freedom stage by introducing a flexible structure to develop a middle-range six-degrees-of-freedom stage. The proposed system provides linear displacements along three axes and rotation motion about three axes. The experimental results indicate that the stage's displacement was 20 mm along the *X*-axis, 20 mm along the *Y*-axis, and 5 mm along the *Z*-axis. The rotation angle around the *X*-axis (θ_x), *Y*-axis (θ_y), and *Z*-axis (θ_z) were all 10 arcsec. The proposed system can thus provide multi-degree compensation for motion errors and increase the precision of a moving stage. This system can be used for applications such as AFM or SPM systems.

ACKNOWLEDGEMENT

This work was supported by the National Science Council, Taiwan, Republic of China under grant NSC 95–2221-E-150–052.

REFERENCES

1 **Matey, J. R., Crandall, R. S., Brycki, B.,** and **Briggs, G. A. D.** Bimorph-driven x–y–z translation stage for scanned image microscopy. *Rev. Sci. Instrum.*, 1987, **58**, 567–570.

2 **Heil, J., Bohm, A., Primke, M.,** and **Wyder, P.** Versatile three-dimensional cryogenic micropositioning device. *Rev. Sci. Instrum.*, 1996, **67**, 307–311.

3 **Chang, S. H.** and **Du, B. C.** A precision piezodriven micropositioner mechanism with large travel range. *Rev. Sci. Instrum.*, 1988, **69**, 1785–1791.

4 **Chang, S. H., Tseng, C. K.,** and **Chien, H. C.** An ultra-precision XY θ_z piezo-micropositioner. Part I: design and analysis. *IEEE Trans. Ultrason., Ferroelectr. Freq. Control*, 1999, **46**, 897–905.

5 **Chang, S. H., Tseng, C. K.,** and **Chien, H. C.** An ultra-precision XY θ_z piezo-micropositioner. Part II: experiment and performance. *IEEE Trans. Ultrason., Ferroelectr. Freq. Control*, 1999, **46**, 906–912.

6 **Jywe, W. Y., Liu, C. H.,** and **Teng, Y. F.** Development of a flexure hinge-based stack-type 5 DOF nanometer-scale stage for a heavy-loading machining process. *Proc. IMechE, Part B: J. Engineering Manufacture*, 2006, **221**(B3), 379–385. DOI: 10.1243/09544054JEM1487.

7 **Jywe, W. Y., Jeng, Y. R., Teng, Y. F., Wu, C. H., Wang, H. S.,** and **Chen, Y. J.** A novel 5 DOF thin coplanar nanometer-scale stage. *Precis. Engng*, 2008, **32**, 239–250.

8 **Holmes, M., Hocken, R.,** and **Trumper, D.** The long-range scanning stage: a novel platform for scanned-probe microscopy. *Precis. Engng*, 2000, **24**, 191–209.

9 **Egashira, Y., Kosaka, K., Takada, S., Iwabuchi, T., Baba, T., Moriyama, S., Harada, T., Nagamoto, K., Nakada, A., Kubota, H.,** and **Ohmi, T.** 0.69 nm resolution ultrasonic motor for large stroke precision stage. In Proceedings of *IEEE NANO*, 2001, pp. 397–402 (IEEE, Piscataway, New Jersey).

10 **Shutov, M. V., Howard, D. L., Sandoz, E. E., Sirota, J. M., Smith, R. L.,** and **Collins, S. D.** Electrostatic inchworm microsystem with long range translation. *Sens. Actuators A:, Phys.*, 2004, **114**, 379–386.

11 **Chu, C. L.** and **Fan, S. H.** A novel long-travel piezo-electric-driven linear nanopositioning stage. *Precis. Engng*, 2006, **30**, 85–95.

12 **SIOS Me.** β echnik GmbH, Catalog, available from http://www.sios.de.